Electronic Supplementary Material (ESI) for Journal of Materials Chemistry A.

Supplementary Information

Surfactant Effects on Synthesis of Porous Cerium Oxide from a Type IV Deep Eutectic Solvent

Iva Manasi,*[a] Mohammad R. Andalibi,[b] Rémi Castaing,[c] Laura Torrente Murciano[b] and Karen J. Edler*[a]

[a] *Department of Chemistry, University of Bath, Claverton Down, Bath BA2 7AY, UK; E-mail: im554@bath.ac.uk, k.edler@bath.ac.uk*

[b] *Department of Chemical Engineering and Biotechnology, West Cambridge Site, Philippa Fawcett Drive, Cambridge, CB3 0AS, UK.*

[c] *Material and Chemical Characterisation Facility, University of Bath, Claverton Down, Bath, BA2 7AX, UK.*

XRD from Ceria Samples

PXRD from the various ceria samples show peaks corresponding to the Bragg reflections from the different crystal lattices (Figure 1). These diffraction peaks in the angular range covered by the experiment ($2\theta = 20 - 90°$) were: {111}, {200}, {220}, {311}, {222}, {400}, {331}, {420} and {422}. The average crystallite size was determined by applying the Scherrer equation [1] for all peaks that a Lorentzian function was fitted to and averaging them. The crystallite size calculated for each of the diffraction directions is similar to the average value, indicating the poly-crystallite nature of the structures.

Table S1 and S2 summarize the XRD data for ceria samples made from DES without and with added water, respectively, and with 20% w/w added surfactants. The tables summarize the average position of the various diffraction peaks and the corresponding crystal lattice size along with the standard deviation error for the different samples.

Table S1: Scherrer crystallite size corresponding with XRD data for ceria samples synthesised from Ce:U DES without added water

	d (nm)									
	{111}	{200}	{220}	{311}	{222}	{400}	{331}	{420}	{422}	Average
$2\theta(°)$	28.49	33.03	47.36	56.23	58.99	69.32	76.54	78.95	88.31	
CeOx	25.94	32.05	30.21	28.52	28.90	37.38	32.04	32.58	35.05	31.41 ± 3.28
$C_{16}TAB$	25.94	26.23	27.46	28.51	24.42	33.58	39.10	39.75	42.81	31.98 ± 6.58
$C_{12}TAB$	25.94	26.23	27.43	28.51	28.89	30.58	39.11	39.82	42.82	32.15 ± 6.18
$BrijC_{10}$	25.94	26.22	27.46	28.51	28.89	30.57	39.16	39.83	35.07	31.30 ± 5.08
$C_{12}TANO_3$	25.94	26.22	30.21	28.49	45.40	30.57	32.04	35.84	42.80	33.06 ± 6.57
$C_{16}TANO_3$	25.94	28.85	27.46	34.85	28.89	44.84	32.04	35.84	42.85	33.51 ± 6.34

The samples labelled as surfactants are made from Ce:U DES + 20% w/w of corresponding surfactant.

Table S2: Scherrer crystallite size corresponding with XRD data for ceria samples synthesised from Ce:U DES with added water

	d (nm)									
	{111}	{200}	{220}	{311}	{222}	{400}	{331}	{420}	{422}	Average
$2\theta(°)$	28.46	33.02	47.41	56.25	59.03	69.28	76.67	78.97	88.28	
5W	21.95	22.19	23.23	28.52	35.31	37.33	27.08	35.81	42.81	30.47 ± 7.15
$C_{16}TAB$	25.93	22.19	23.23	24.11	37.39	37.33	27.11	39.85	35.02	30.24 ± 6.64
$C_{12}TAB$	21.95	26.23	23.24	24.13	34.67	37.38	35.35	42.14	45.36	32.27 ± 8.17
$BrijC_{10}$	28.54	32.05	33.57	34.85	37.39	33.63	39.16	35.85	42.83	35.32 ± 3.92

The sample labelled as 5W is made from Ce:U DES+5W and the ones labelled as surfactants are made from Ce:U DES+5W with 20% w/w added corresponding surfactant.

SEM and TEM Images from Ceria Samples

Representative SEM and TEM images for ceria samples made from Ce:U DES without and with 20% w/w are shown in Figure S1 & S2, respectively. The SEM data shown here was collected at a magnification of 10000× and the TEM data at two magnifications is shown, 250000× (Figure S2(a)) and 1500000× (Figure S2(b)).

Also shown here in Figure S3 are representative SEM images, collected at a magnification of 20000×, for ceria samples made from CE:U DES with 5 moles of added water (DES+5W) without and with 20% w/w surfactants (C_{16}TAB & BrijC_{10}).

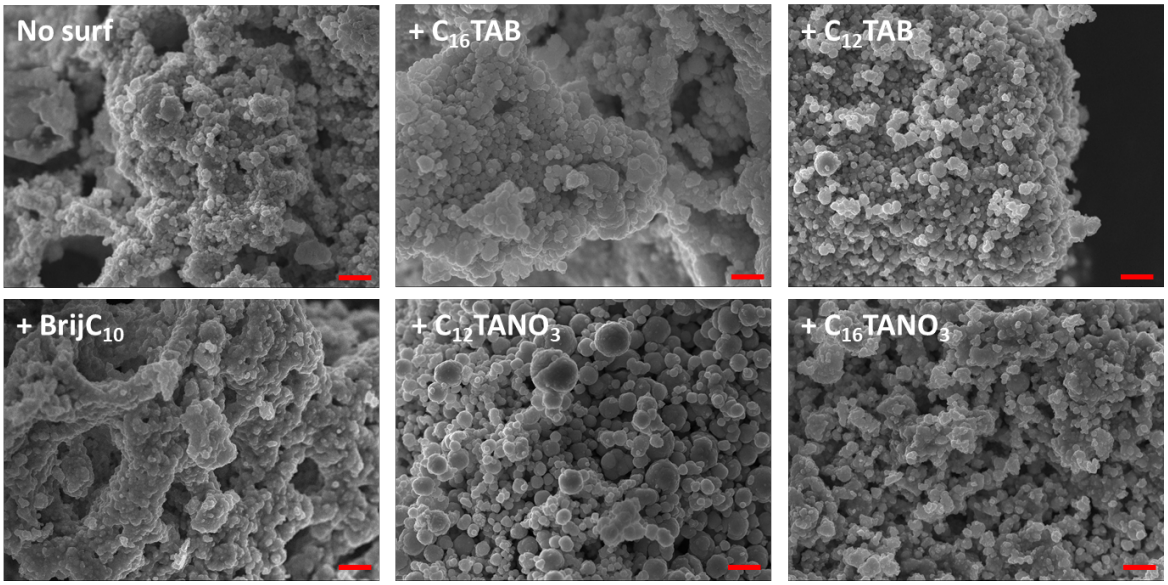

Figure S1: Representative SEM images of ceria samples, made from Ce:U DES without and with added surfactants (20% w/w), after calcination (scale bars depict 1 μm.).

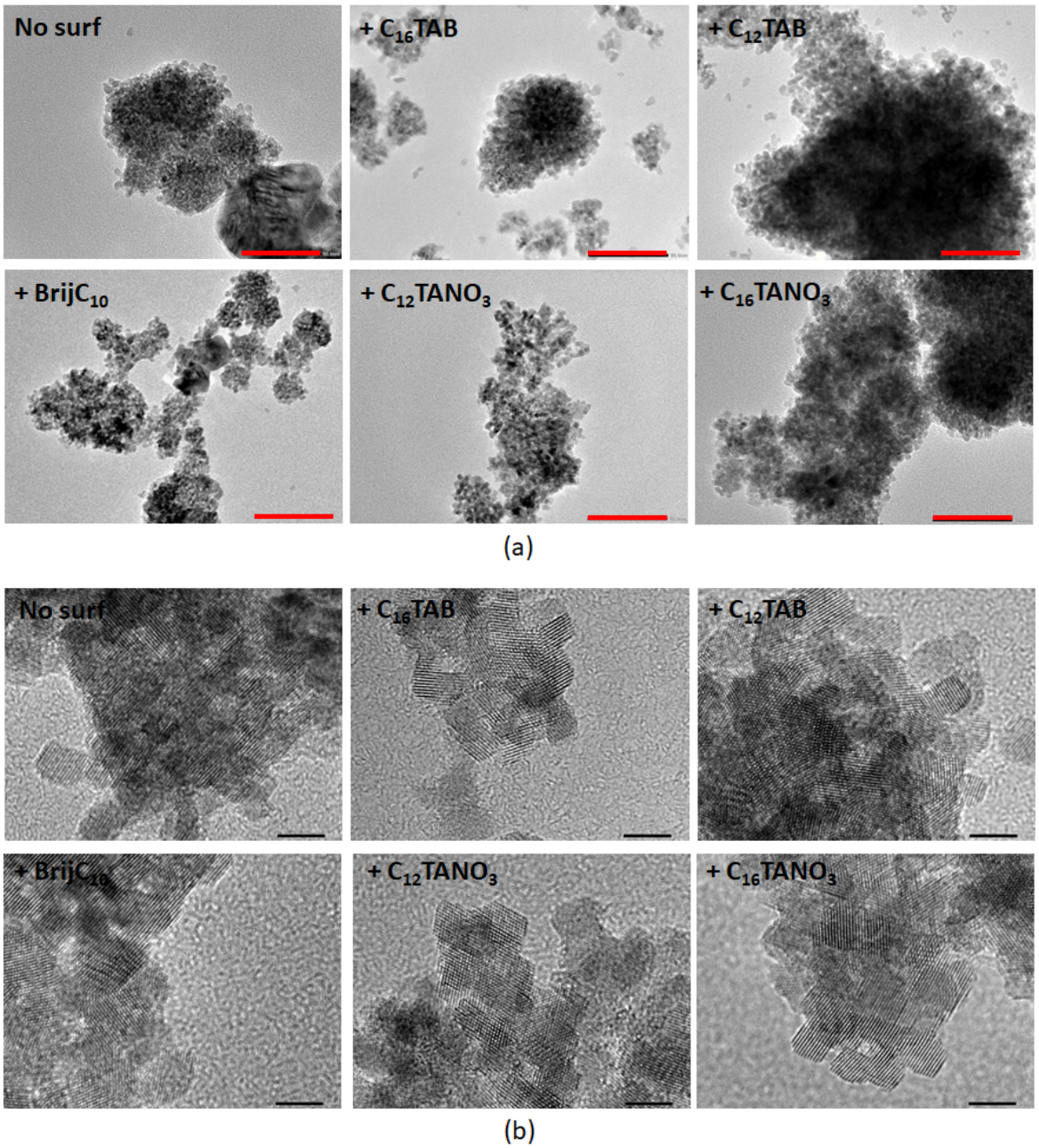

Figure S2: Representative TEM images of ceria samples, made from Ce:U DES without and with added surfactants (20% w/w), after calcination at 2 magnifications: (a) 250000× (scale bars depict 50 nm.) and; (b) 1500000×.(scale bars depict 5 nm.)

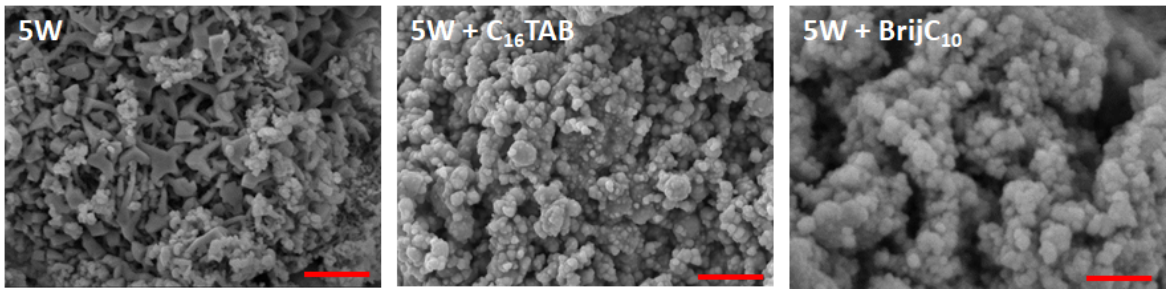

Figure S3: Representative SEM images of ceria samples, made from Ce:U DES with water (molar ratio 1:5) and added surfactants (20%w/w), after calcination (scale bars depict 1 μm.).

CO Oxidation – Arrhenius Plots

Here we present the Arrhenius plots over the full range ($0 - > 85\%$ conversion range; Figure S4(a)) and $5 - 15\%$ conversion range (Figure S4(b)) for sample +20% $C_{12}TANO_3$ at three different GHSVs: 1350, 2160 and 2700 $NmL_{CO}/g_{catalyst}.h$; which are then used to calculate the apparent activation energy (E_a). The same method is applied for all samples and the E_a values are within 10% of the average value, as reproducible as typically reported in the literature. [2]

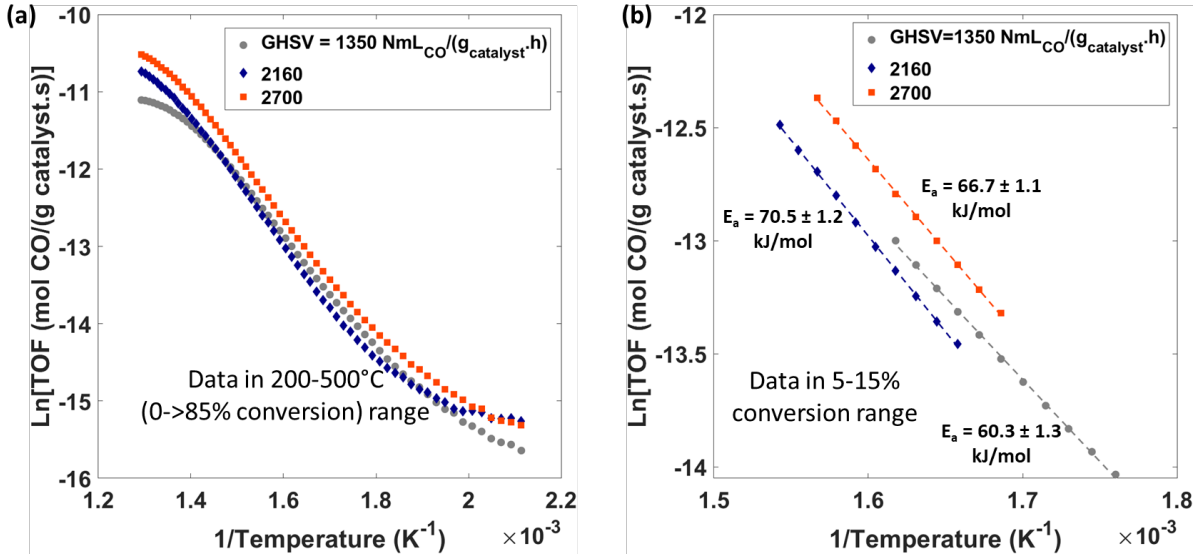

Figure S4: Arrhenius plots over the full range (a) and $5 - 15\%$ conversion range (b) on sample +20% $C_{12}TANO_3$ at three different GHSVs.

XPS from Ceria Samples

XPS measured from the different ceria samples shows a surface composition of cerium, oxygen and carbon with the presence of both Ce^{3+} and Ce^{4+} valence state of the cerium atom. The percentage concentration of Ce^{3+} is $12 - 20$ % of the total amount, with CeOx made from DES without added surfactant showing the lowest Ce^{3+} percentage followed by the C12-surfactant templated ceria (C_{12}TAB, followed by BrijC_{10} followed by $C_{12}TANO_3$) and finally the C_{16}TAB templated ceria. Figure S5 shows the specific reaction rate as a function of the Ce^{3+} ($Ce^{3+}/(Ce^{3+}+Ce^{4+})$ percentage determined by XPS for the different ceria samples. The specific rate of the reaction, and therefore the activity, does not follow the trend expected from the literature [3] of increasing activity with increasing Ce^{3+} ratio in the surface composition. This could be due to the influence of other factors, namely an increase in surface area leading to higher activity and halide poisoning of the catalytic sites reducing the activity, as discussed in the main text. Both C_{12}TAB and C_{16}TAB templated ceria contain halides which poison the catalytic activity and reduce the activity compared to the non-templated ceria and therefore despite an increase in the Ce^{3+} percentage, the specific reaction rate is lower for these samples compared to the non-templated ceria. In the case of BrijC_{10} and $C_{12}TANO_3$, the increase in surface area is the dominating factor leading to an increase in the activity (also reflected in the higher specific reaction rate), as opposed to the Ce^{3+} percentage.

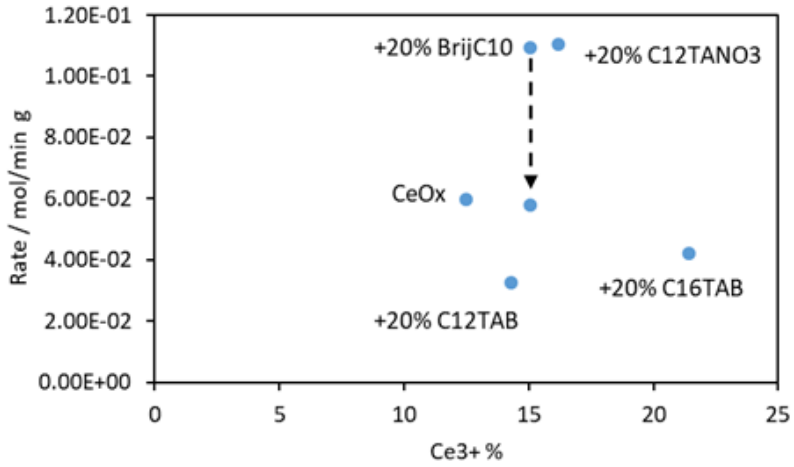

Figure S5: Specific reaction rate per gram for the catalytic conversion reaction as a function of the Ce^{3+} percentage determined by XPS for the different ceria samples.

For ceria templated from BrijC_{10}, we see a drop in activity from the first to consecutive runs (indicated by the arrow in Figure S5). This potentially arises from a bimodal porosity distribution in these non-ionic surfactant templated ceria; microporosity due templating from the non-ionic head group and mesoporosity because of templating from the micelles. We suggest

that the micropores are blocked in the initial CO oxidation run and therefore we see a drop in the catalytic activity in subsequent runs.

References

[1] P. Scherrer. *Bestimmung der inneren Struktur und der Größe von Kolloidteilchen mittels Röntgenstrahlen*, pages 387–409. Springer Berlin Heidelberg, Berlin, Heidelberg, 1912.

[2] Eleonora Aneggi, Jordi Llorca, Marta Boaro, and Alessandro Trovarelli. Surface-structure sensitivity of co oxidation over polycrystalline ceria powders. *Journal of Catalysis*, 234:88–95, 2005.

[3] Jose Manuel López, Alexander L. Gilbank, Tomás García, Benjamín Solsona, Said Agouram, and Laura Torrente-Murciano. The prevalence of surface oxygen vacancies over the mobility of bulk oxygen in nanostructured ceria for the total toluene oxidation. *Applied Catalysis B: Environmental*, 174-175:403–412, 2015.